ELSEVIER

Journal of Chromatography A, 734 (1996) 319–330

JOURNAL OF CHROMATOGRAPHY A

Investigation of matrix effects in capillary zone electrophoresis

J. Boden, K. Bächmann*

Fachbereich Chemie der Technischen Hochschule Darmstadt, Petersenstr. 18, D-64287, Darmstadt, Germany

Received 10 August 1995; revised 27 November 1995; accepted 4 December 1995

Abstract

The theoretical principles used in the explanation of the separation process in capillary zone electrophoresis (CZE), during the analysis of samples with different matrix cases, are discussed. At the beginning of the CZE separation, an isotachophoretic (ITP) process takes place between the matrix ion and the electrolyte co-ion (ITP range). As a result of the ITP effect, analytes with mobilities between those of the matrix ion and the co-ion, show increasing peak heights with increased matrix concentration whereas for slower or faster analytes peak-broadening occurs. By adding a second matrix ion to the sample, the ITP range can be shifted, so that analyte ions are determined which otherwise could not be analyzed. A further established matrix effect is the shift of the migration times. The reliability of the anticipated effects was investigated for inorganic anions, using several electrolytes and matrix ions.

Keywords: Matrix effects; Sample self-stacking; Isotachophoretic initial state; Inorganic anions

1. Introduction

The determination of inorganic ions in the presence of matrices is a fundamental analytical problem. There are only a few publications where the application of capillary zone electrophoresis (CZE) separation to samples containing matrices was investigated [1–6].

In principle, the matrices can be classified in non-charged and in charged species. The advantage of a sample with a non-charged matrix is the low conductivity of such samples, because the neutral species have no influence on the ionic strength of the sample. Therefore, the stacking effect during the initial state of the CZE separation which can be obtained in aqueous samples with low conductivity [7–9] can also take place in the presence of a neutral matrix (see Fig. 1a). This focusing effect leads to small analyte zones in the initial state of the electrophoretic separation, resulting in high plate numbers for the analyte peaks in the electropherogram.

Furthermore, all on-line preconcentration methods that were developed for the improvement of the detection limits of anions in aqueous solutions, like electrokinetic injection, electrokinetic injection with an isotachophoretic (ITP) state and sample stacking, can be transferred to samples with a neutral matrix. Taking some special facts into consideration, such as the change of viscosity and pH of the sample in the presence of a neutral matrix, the samples can be determined without problems up to high analyte-to-matrix ratios, by applying an on-line process to remove the matrix [6].

The analysis of samples with an ionic matrix, however, is a more complicated problem. Excess of an ion leads to a high electric conductivity of the

*Corresponding author.

0021-9673/96/$15.00
SSDI 0021-9673(95)01314-8

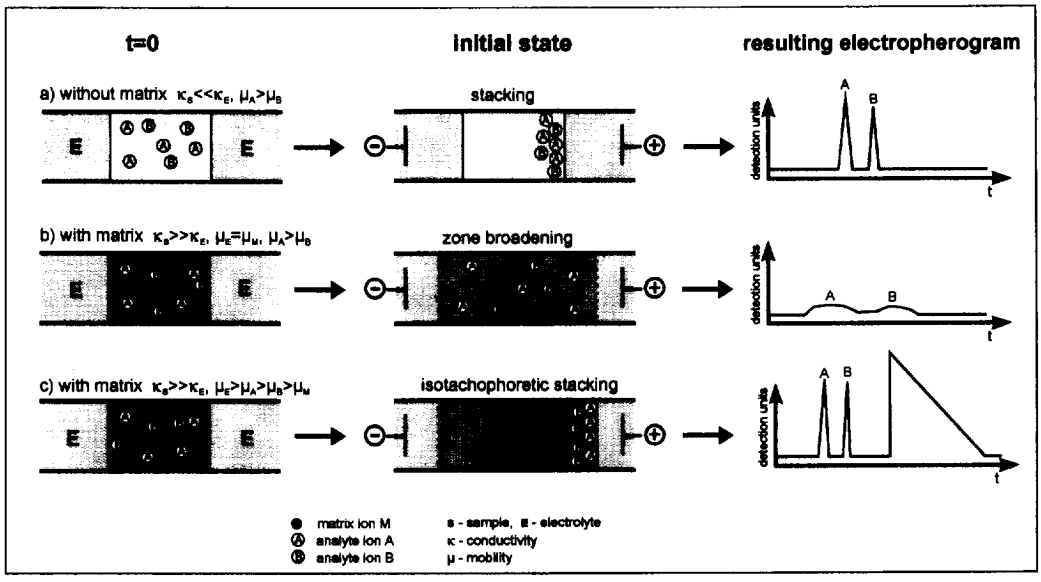

Fig. 1. Influence of the sample contents on the stacking process and the resulting electropherograms.

sample that is dependent on the mobility and the concentration of the matrix ion (see Eq. 1 in Table 1). For a sample conductivity higher than the conductivity of the electrolyte, the velocity of the analyte ions in the electrolyte is higher than in the sample zone. Therefore, in contrast to samples with low conductivity (Fig. 1a), zone broadening takes place, resulting in flat peaks with low plate numbers and poor resolution (see Fig. 1b). Furthermore, on-line preconcentration methods such as electrokinetic injection or sample stacking are not applicable because of the unfavourable ratio of conductivity and field strength, respectively. However, the use of hydrostatic or hydrodynamic injection results in higher limits of detection.

A possible method for preconcentrating analyte ions in the presence of an ionic matrix is the use of an ITP process, before the CZE separation.

Some methods for coupling a precolumn for ITP and a separation capillary for CZE are described in the literature [10–15]. These arrangements require expensive equipment and often require a second detector. Furthermore, the coupling of two capillaries is difficult to use in routine analysis. The disadvantages of the coupling of ITP and CZE do not exist if the ITP and CZE states take place in the same capillary. This can be realized by creating an ITP step in the initial state of a CZE separation, using the matrix ion as one part and the electrolyte co-ion as the other part of the ITP system.

A theoretical description of the processes occuring in the presence of a high mobile matrix ion was given by Beckers and Everaerts [16] and Gebauer et al. [1]. Foret et al. [14] described a procedure to employ ITP and CZE in the same capillary, using an excess of the high mobile chloride ion in the sample acting as a leading electrolyte, for the separation of a standard protein mixture.

It was also shown that for a low mobile matrix ion, an ITP state can occur using the matrix ion as the terminator and the co-ion of the electrolyte as the leading component [3].

Therefore, it can be assumed that an ionic matrix can be applied as either the leading or the terminating ion in the initial state of the CZE-separation, in dependence of its mobility. Three cases can be distinguished; a low mobile matrix ion, a high mobile matrix ion and a combination of two matrix ions. The electrolyte for CZE should have a selected mobility and concentration so that it can act as the corresponding (terminating or leading) ion. The ITP mode ends when the concentration of the matrix ion

is decreased due to its electromigrative dispersion. After that, the analytes can be de-stacked, one after the other, and migrate into the CZE mode.

At the end of the analysis, the analytes with mobilities ranging between those of the matrix ion and the co-ion are preconcentrated resulting in sharp peaks with high plate numbers as can be seen in Fig. 1c.

Peak-broadening results for analytes with mobilities outside the mobility range between the co-ion and the matrix ion. This requires that the electrolyte co-ion should be chosen so that the highest possible number of analytes is lying in the considered ITP range.

Furthermore, it should be possible to focus analytes subjected to peak-broadening by adding a second matrix ion to the sample. Then, two ITP states could be realized simultaneously and the electrolyte co-ion could have an intermediate mobility.

In this paper, the influence of the initial ITP state on the concentration effect and on the shift of the migration times will be discussed. Furthermore, the anticipated effects will be investigated practically, for the determination of inorganic anions in the presence of several matrices.

2. Theoretical

2.1. Mechanism of the separation in the presence of an ionic matrix

The movement of the different zones in the presence of a matrix ion can be subdivided into four successive steps; the migration of analytes and matrix ions from the sample zone to the boundary of the sample zone and the electrolyte zone, the regulation of the concentrations at this boundary, the ITP mode and finally, the de-stacking of the analytes resulting in their transition to the CZE mode.

A detailed description of this mechanism for all three matrix cases can be given as follows:

After injection, the sample zone is a homogeneous mixture of the analyte A and the matrix ion M (see Fig. 2a), with the electric conductivity κ_S (see Table 1, Eqs. 1 and 2). On applying an electric field, the matrix and analyte ions migrate from the sample

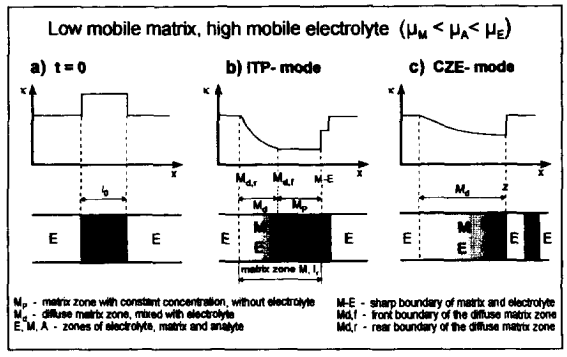

Fig. 2. Scheme showing the development of the ITP stacking process in the presence of a low mobile matrix ion.

zone to the boundary of the sample zone and the electrolyte zone with the velocity $v_{i,j}$ (in this case the indices j and i stand for the zone and for the species, respectively).

$$v_{i,j} = \frac{i \cdot \mu_i}{\kappa_j} \tag{3}$$

Reaching this boundary the concentration of the different species i is regulated according to the Kohlrausch-regulating-function (Eq. 4) [17,18],

$$c_{i,r} = c_E \cdot \frac{\mu_i \cdot (\mu_E + \mu_C)}{\mu_E \cdot (\mu_i + \mu_C)} \tag{4}$$

resulting in the typical ITP profile of conductivity and concentration (see Fig. 2b). Assuming that the concentration of the matrix ion in the sample zone $c_{M,S}$ is higher than the concentration of the co-ion c_E a diluted pure matrix zone with the length l_r results.

$$l_r = l_0 \cdot \frac{c_{M,S}}{c_{M,r}} \tag{5}$$

In the case of a low mobile matrix and a high mobile co-ion (see Fig. 2), a self-sharpening effect at the front of the matrix zone leads to a sharp boundary M-E between the matrix and the electrolyte. In contrast, for a high mobile matrix and a low mobile co-ion, the self-sharpening effect takes place at the rear side of the matrix zone (data not shown). In both cases the analytes are stacked isotachophoretically on the sharp boundary between the electrolyte and matrix zones. The highest attainable stacking concentration is also given by the

Table 1
Summary of the equations for different matrix cases [1,15,19]

	Low mobile matrix $\mu_E > \mu_A > \mu_M$	High mobile matrix $\mu_M > \mu_A > \mu_E$	Two matrices M1 and M2 $\mu_{M1} > \mu_E > \mu_{M2}$		
Conductivity of the sample zone κ_S	$\kappa_S = F \cdot c_{M,0} \cdot (\mu_M + \mu_G)$ (1)		$\kappa_S = F \cdot [c_{M1,0}(\mu_{M1} + \mu_G) + c_{M2,0}(\mu_{M2} + \mu_G)]$ (2)		
			Matrix M1:	Matrix M2:	
Loss of concentration plateau of the matrix t_X	$t_X = \frac{l_0 \cdot \kappa_S}{i \cdot (\mu_E - \mu_M)}$ (8)	$t_X = \frac{l_0 \cdot \kappa_S}{i \cdot (\mu_M - \mu_E)}$ (9)	$t_{X1} = \frac{l_0 \cdot \kappa_S}{i \cdot (\mu_{M1} - \mu_E)}$ (10)	$t_{X2} = \frac{l_0 \cdot \kappa_S}{i \cdot (\mu_E - \mu_{M2})}$ (11)	
			$\mu_A > \mu_E$	$\mu_A < \mu_E$	
ITP time of one analyte A t_{ITP}	$t_{ITP} = \frac{l_0 \cdot \kappa_S \cdot (\mu_E - \mu_M)}{i \cdot (\mu_A - \mu_M)^2}$ (13)	$t_{ITP} = \frac{l_0 \cdot \kappa_S \cdot (\mu_M - \mu_E)}{i \cdot (\mu_M - \mu_A)^2}$ (14)	$t_{ITP} = \frac{l_0 \cdot \kappa_S \cdot (\mu_{M1} - \mu_E)}{i \cdot (\mu_{M1} - \mu_A)^2}$ (15)	$t_{ITP} = \frac{l_0 \cdot \kappa_S \cdot (\mu_E - \mu_{M2})}{i \cdot (\mu_A - \mu_{M2})^2}$ (16)	
			$\mu_A > \mu_E$	$\mu_A = \mu_E$	$\mu_A < \mu_E$
Migration time of one analyte A t_m	$t_m = \frac{i_D}{v_{A,E}} - \frac{l_0 \cdot \kappa_S \cdot (\mu_E - \mu_M)}{i \cdot \mu_M \cdot (\mu_A - \mu_M)}$ (19)	$t_m = \frac{i_D}{v_{A,E}} - \frac{l_0 \cdot \kappa_S \cdot (\mu_M - \mu_E)}{i \cdot \mu_M \cdot (\mu_M - \mu_A)}$ (20)	$t_m = \frac{i_D}{v_{A,E}} - \frac{l_0 \cdot \kappa_S \cdot (\mu_{M1} - \mu_E)}{i \cdot \mu_{M1} \cdot (\mu_{M1} - \mu_A)}$ (21)	$t_m = \frac{i_D}{v_{A,E}}$ (22)	$t_m = \frac{i_D}{v_{A,E}} - \frac{l_0 \cdot \kappa_S \cdot (\mu_E - \mu_{M2})}{i \cdot \mu_{M2} \cdot (\mu_A - \mu_{M2})}$ (23)

Kohlrausch-regulating-function (Eq. 4) [17,18]. During the ITP mode, the analyte zone as well as the electrolyte and the matrix ions migrate with the same ITP velocity v_{ITP}.

$$v_{ITP} = v_{A,A} = v_{M,M} = v_{E,E} = \frac{i \cdot \mu_A}{\kappa_A} = \frac{i \cdot \mu_M}{\kappa_M} = \frac{i \cdot \mu_E}{\kappa_E} \quad (6)$$

In contrast with the sharp boundary, the other side of the matrix zone is a diffuse one. Within this diffuse matrix zone M_d, the concentration and the conductivity are not stationary due to the increasing concentration ratio of electrolyte to matrix depending on time and position. The change of concentration and conductivity can be described using the theory of electromigrative dispersion resulting in a root-function [19]. According to this theory, a convex profile for both matrix concentration and conductivity will be received in the case of a low mobile matrix and a high mobile electrolyte. Therefore, the matrix peak of a low mobile matrix obtained in the electropherogram will be concave (''tailing''). In contrast, the shape of a high mobile matrix will be convex (''fronting'') in the electropherogram.

The zone boundary between the diffuse matrix zone M_d and the matrix zone with the concentration plateau M_P moves with the velocity v_{M-M}, whereas the velocity of the boundary of the diffuse zone and the electrolyte zone can be described using v_d [13,15].

$$v_{M-M} = \frac{i \cdot \mu_E}{\kappa_M} \quad v_d = \frac{i \cdot \mu_M}{\kappa_E} \quad (7)$$

Due to the different velocity v_{M-M} in comparison to the ITP velocity v_{ITP} of the sharp boundary M-E of the non-diffuse matrix zone (see Eq. 6), a loss of the non-diffuse matrix zone results at the time t_X.

Assuming that at the beginning of the separation the distance of the two boundaries conforms with the length of the regulated matrix zone l_r and using Eqs. 1–5, the time of their coincidence t_X can be calculated for the different matrix cases according to Eqs. 8–11 (see Table 1).

After the time t_X, the self-sharpening effect of the sharp boundary takes place, but no stationary conditions now exist due to the continuous change of the concentration ratio of the electrolyte and matrix ions c_E/c_M resulting also in a change in the electric conductivity.

Therefore, the velocity of the sharp boundary M-E also changes continuously. The value of the concentration and of the conductivity of M-E can be calculated according to the equations describing electrodispersion [19]. The analytes are in stack on M-E until the time t_{ITP} at which the velocity of the boundary $M - E$ v_{M-E} [1,19] is equal to the velocity of the analytes in the electrolyte $v_{A,E}$ (see Eq. 3, in this case the index E stands for the electrolyte zone) according to:

$$\sqrt{\left(v_{M,E} \cdot \frac{x_{M-E}}{t_{ITP}}\right)} = \frac{i \cdot \mu_A}{\kappa_E} \quad (12)$$

Insertion of x_{M-E} [1,15,19] and transformation leads to the equations for the ITP time (see Eqs. 13–16, Table 1). It can be seen that the ITP time of the analytes for all three matrix cases depends on the mobility difference of the matrix and analyte as well as of the matrix and co-ion. Furthermore, the ITP time is connected to the length of the sample zone, the conductivity of the sample zone (and therefore, also to the matrix concentration) and the concentration of the co-ion (contained in the current density, i).

After the de-stacking procedure the analytes migrate into the CZE-mode (see Fig. 2c) with its normal electrophoretic velocity $v_{A,E}$ (see Eq. 3).

2.2. Summary of the expected matrix effects

Due to the described on-line coupling of ITP and CZE, some matrix effects result, such as the ITP stacking, the shift of the migration times, the change in the resolution and the increased influence of contaminations of the electrolyte system.

The most important matrix effect is the ITP stacking of the analytes. The attainable stacking factors can be calculated according to the Kohlrausch-regulating-function (see Eq. 4).

Another matrix effect is the shift of the migration times. This effect can be explained by the velocity of the analytes during the ITP mode compared to the usual CZE-mode. The migration time t_m to the detector point l_d can be obtained from the sum of the ITP-time and the CZE-time of one analyte.

$$t_m = t_{CZE} + t_{ITP} \quad (17)$$

$$t_m = \frac{l_d - l_{ITP}}{v_{A,E}} + t_{ITP} \quad (18)$$

Insertion of t_{ITP} (Eqs. 13–16) and transformation leads to the equations for the migration times (see Eqs. 19–23). It is obvious from these equations that the migration times are influenced in a different way for the different matrix cases. For low mobile matrices, a shortening of the migration times will be obtained. In contrast, a high mobile matrix leads to longer migration times. In the presence of two matrices, no uniform shift of the migration times of the analytes exists. Depending on the mobility difference between the analyte and the electrolyte co-ion, different equations have to be used for the calculation of the t_m values (see Table 1, Eqs. 21–23). From these equations, it can be concluded that analytes with a higher mobility than the electrolyte co-ion are slowed down, whereas analytes with a lower mobility are accelerated. As the result of this contrasting influence of the ITP state on the whole electropherogram, the analyte peaks come closer together.

In contrast to CZE in the pure ITP mode, the analyte zones are not separated from one another by the electrolyte. This fact leads to worse resolution of the peaks in the electropherogram with an increased influence of the ITP state. Over long ITP times, some analytes reach the detector point still in stack and cannot be detected as single peaks.

In addition, the purity of the electrolyte plays a more important role than in the normal CZE mode. In principal, all ions contained in the electrolyte with mobilities between the matrix ion and the electrolyte co-ion can be stacked into the sample zone during the ITP state and appear as a peak in the electropherogram. Therefore, the purity of the applied electrolytes should be examined before using them for the determination of analytes in the presence of ionic matrices.

3. Experimental section

For our investigations, laboratory-built CZE equipment as well as the automatic CZE device P/ACE system 2050 from Beckman (München, Germany) were used.

The separations were carried out using conventional untreated fused-silica capillaries (50 and 75 μm I.D.) from CS-Chromatographie Service (Langerwehe, Germany).

For the home-made CZE device, the capillaries passed through an ABI 785A programmable absorbance detector (Applied Biosystems, Weiterstadt, Germany) with variable wavelength, and its outlets were placed in two 10-ml electrolyte vials.

The high voltage from a 30 kV power supply (F.u.G. Electronic, Rosenheim, Germany), used in the negative voltage mode, was applied between the two ends of the capillary with platinum–iridium electrodes dipping into the electrolyte vials.

The absorbance units of the home-made detector were transformed by an A/D board (ERC, Alteglofsheim, Germany) into μV, hence the output of the data was in the voltage mode. The electropherograms were evaluated using APEX chromatography software (Autochrom, Milford, MA, USA). The electric conductivity of the sample solutions were measured with an LF92 conductometer (WTW, Weilheim, Germany).

3.1. Chemicals

All solutions, electrolytes and standards were prepared using water purified with a Milli-Q system (Millipore, Eschborn, Germany). All reagents were of analytical-reagent grade and were obtained from Merck (Darmstadt, Germany). To shorten the analysis time for the determination of anions the EOF modifiers tetradecyltrimethylammoniumhydroxide (TTAOH) or dodecyltrimethylammoniumhydroxide (DoTAOH) were added to the electrolyte. Both were laboratory-made [25] from their bromide salts, using the anion exchange material Amberlite IRA-904 (Serva, Heidelberg, Germany).

4. Results and discussion

In order to detect the UV-inactive ions, the indirect UV-detection mode using a UV-active background electrolyte should be applied [20–27]. Measuring several inorganic and organic anions in the presence

of different matrices, different electrolytes must be used to change the ITP range. In Table 2, the mobilities of some electrolyte co-ions and selected analyte ions are summarized.

4.1. Electrolyte and matrix ion with similar mobilities

The most unfavourable matrix effect is obtained if the matrix anion and the electrolyte co-ion have similar mobilities. In this case, no ITP state is available and peak-broadening for all analytes occurs (see Fig. 1b).

This can be the case if, for example, the matrix ion and the electrolyte co-ion are identical species. Fig. 3 shows four electropherograms with molybdate as the electrolyte co-ion and with different concentrations of molybdate in the sample. All analyte ions are broadened and therefore the peak heights decrease as can be seen in Fig. 3b. Even at low molybdate concentrations (2 m*M*) or low analyte-to-matrix ratios (1:80), a reduction of the peak heights occurs. The peak area for every analyte ion is constant up to a molybdate concentration of 10 m*M*. At higher concentrations, the peak areas also decrease.

Furthermore, it can be seen that nitrate was directly detected due to its higher absorbance compared to the molybdate electrolyte, hence, the nitrate peak was in the opposite direction. For all other ions the indirect detection mode obtained.

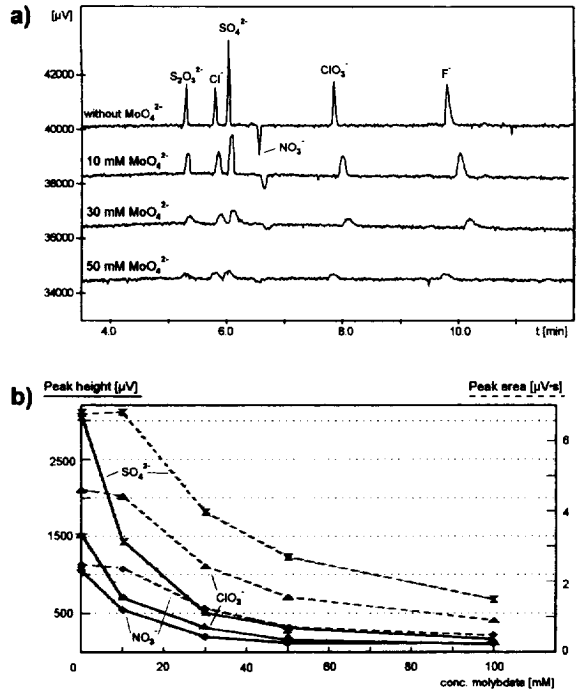

Fig. 3. The influence of a molybdate matrix in the sample on the electropherograms using molybdate as the electrolyte also. (a) Electropherograms for different matrix concentrations. (b) Peak heights vs. concentration of molybdate in the sample. Electrolyte, 5 m*M* sodium molybdate, pH 6.7; analytes, 50 μM each; capillary, 70 cm to the detector, 86 cm total length, 50 μm I.D; detection, indirect UV (direct UV detection for nitrate), 211 nm; injection, hydrostatic (10 cm, 30 s); device, laboratory-built.

4.2. High mobile electrolyte and low mobile matrix ion

Table 2 shows that chromate can be used as a high mobile electrolyte for indirect UV detection [3,26,27]. In samples with fluoride as a slow matrix ion, the mobilities of the common inorganic ions (e.g. chloride, sulfate, nitrate and chlorate) lie between the mobilities of chromate and fluoride.

Fig. 4a shows four electropherograms with different fluoride concentrations. As expected, the inorganic ions form sharp peaks because of the ITP initial state, with the exception of thiosulfate which is decreased due to its higher mobility compared to chromate.

Table 2
Theoretical [28] and effective mobilities of some analyte ions and electrolyte co-ions

	Electrolyte co-ion			Analyte ion					
	Chromate	Molybdate	Salicylate	Chloride	Sulfate	Nitrate	Chlorate	Fluoride	Acetate
μ_{theo} [cm^2/V·s]·10^{-4}	8.8	7.4	3.7	7.9	8.2	7.4	6.7	5.7	4.2
μ_{eff}[a] [cm^2/V·s]·10^{-4}	8.1	7.3	3.5	7.8	7.4	7.3	6.5	5.5	3.9

[a] The effective mobilities were calculated from the electropherograms in the absence of matrix in Figs. 3–5

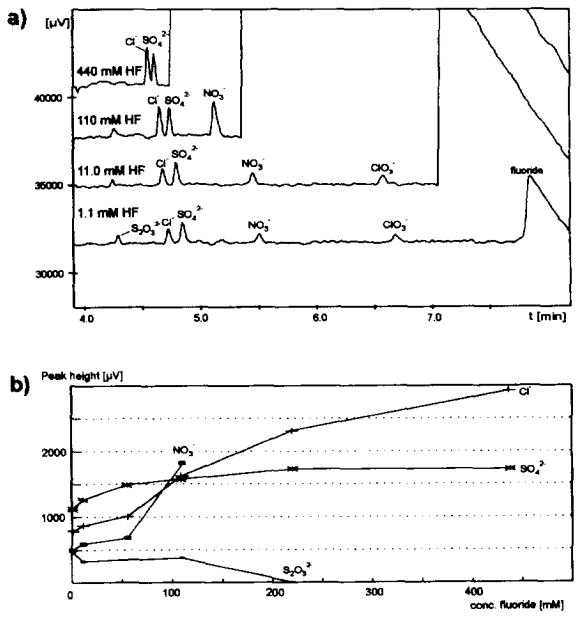

Fig. 4. The influence of a fluoride matrix on the electropherograms using a chromate electrolyte. (a) Electropherograms; (b) peak heights vs. concentration of fluoride. Electrolyte, 5 m*M* potassium chromate, 0.15 m*M* TTAOH, pH 8.4; analytes, 25 μM each; capillary, 65 cm to the detector, 80 cm total length, 75 μm I.D.; detection, indirect UV, 254 nm; device, laboratory built.

With increasing matrix concentration, the analyte ions were overlapped one another by the matrix of fluoride. This effect can be explained by the increased time of the ITP state due to the higher matrix concentration $c_{M,S}$. Therefore, the de-stacking times (Eq. 13, Table 1) are increased also and slow analytes still migrate into the ITP stack at the detector position and cannot be detected as single peaks.

Using the experimental conditions described in Fig. 4, chlorate can be determined up to a fluoride concentration of 80 m*M* and for fluoride concentrations above 200 m*M* nitrate cannot be separated from fluoride.

Furthermore, it can be seen from Fig. 4a that the migration times of the analytes are shortened by increasing the matrix concentration. This fact corresponds to the expectations of the theoretical abstracts given above.

Furthermore, it is observed that with increasing fluoride concentration the peak widths decrease whereas the peak resolution is worsened (The resolution of chloride and sulfate in the presence of 110 m*M* fluoride is 1.2, whereas at 400 m*M* fluoride the resolution is decreased to 1.1).

In Fig. 4b, the peak heights of the analyte ions obtained with different fluoride concentrations are shown. The peak heights were chosen for the evaluation of all peaks because the plate numbers and the peak areas are strongly dependent on the peak shape, which varies for different matrix concentrations. For chloride, sulfate and nitrate, increasing peak heights can be observed. Further enrichment could occur by increasing the concentration of the co-ion (see Eq. 4). Two limitations of the system are caused by the Joule heating and by the linearity range of the detector [3,20].

4.3. Low mobile electrolyte and high mobile matrix ion

In contrast to chromate, a salicylate co-ion has a low mobility, comparable to that of propionate.

Using hydroxide as the high mobile matrix ion, the analyte ions that are faster than the salicylate electrolyte are subjected to an ITP sharpening effect, whereas the less mobile analytes (e.g. propionate) are broadened. In such an electrophoretic system, the hydroxide matrix functions as the leading component whereas salicylate acts as the terminating component during the ITP mode.

Fig. 5a shows three electropherograms of an anion standard with different hydroxide concentrations. The strong growth of the chloride peak that is dependent on the hydroxide concentration can be explained by a chloride contamination of the sodium hydroxide used. The quantification of the blank value of the 400 m*M* hydroxide solution (data not shown) yields a value of $9.5 \cdot 10^{-3}$% (w/w) chloride in the solid sodium hydroxide.

The dependence of the peak heights of some selected ions on the hydroxide concentration is shown in Fig. 5b. As expected, the peak heights of most anions increase with increasing matrix concentration and only the peak heights of propionate are decreased because of its lower mobility compared to the salicylate co-ion. To determine propionate concentration, an electrolyte with lower mobility than salicylate, for instance *p*-aminobenzoate [25], should be chosen.

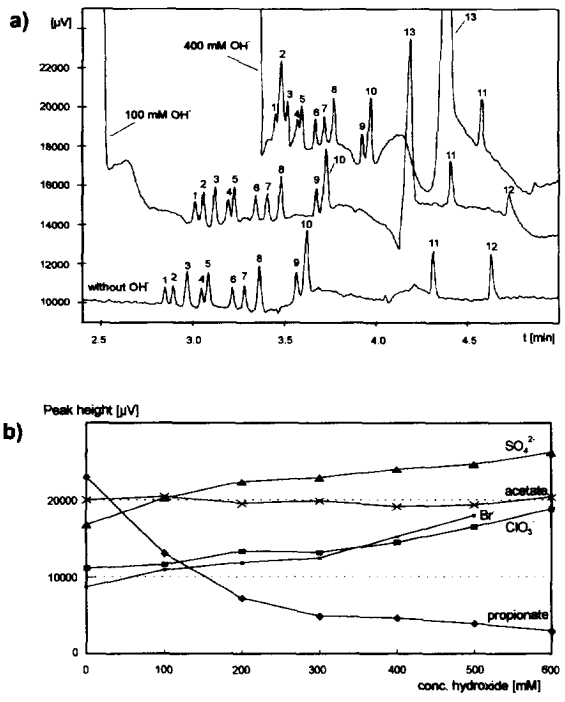

Fig. 5. The influence of a hydroxide matrix on the electropherograms using salicylate as the electrolyte. (a) Electropherograms. (b) Peak heights vs. concentration of hydroxide. Electrolyte, 7.5 m*M* sodium salicylate, 0.1 m*M* TTAOH, pH 8.0; analytes, 25 μM each, 1 = bromide, 2 = chloride, 3 = sulfate, 4 = nitrate, 5 = oxalate, 6 = perchlorate, 7 = chlorate, 8 = malonate, 9 = fluoride, 10 = phosphate, 11 = acetate, 12 = propionate and 13 = carbonate; capillary, 70 cm to the detector, 86 cm total length, 75 μm I.D.; detection, indirect UV, 232 nm; injection, hydrostatic (10 cm, 30 s); device, laboratory-built.

Due to the high mobility difference between acetate and hydroxide, short de-stacking times can be obtained for acetate (see Eq. 14, Table 1), resulting in a nearly independent course of its peak heights and its migration times.

In contrast to the fluoride matrix, where 440 m*M* fluoride was the highest possible matrix concentration, it can be seen that for a hydroxide matrix, single analyte ions can be detected up to a concentration of 600 m*M* hydroxide. This can be explained by the fact that the mobility differences between hydroxide and the analytes are higher than those between fluoride and the analytes. This leads to lower de-stacking times of the analytes in the presence of a hydroxide matrix, resulting in a smaller influence of the ITP state.

In contrast to Fig. 4a, it can be assumed from Fig. 5a that the migration times of the analyte ions are increased by increasing the matrix concentration.

From Fig. 6 it can be seen that the experimental migration times of some selected ions (obtained from Fig. 5a) show good agreement with the theoretical migration times calculated using Eq. 20.

4.4. Addition of a second matrix ion to the sample

Instead of the ITP range bordered by the electrolyte co-ion and the matrix ion, it is possible to create a new ITP range by adding a second matrix ion, with suitable mobility, to the sample. In this way, the ITP system consists of the high mobile matrix zone, M1, and the low mobile matrix zone, M2, in which the M1 zone acts as the leading component and the M2 zone as the terminating electrolyte. Analytes with mobilities between those of the two matrix ions are focussed on the boundary M1-M2. After the loss of the concentration plateaus of the matrices, the analytes with mobilities higher than the co-ion migrate in stack on the rear side of the high mobile matrix zone, whereas analytes with lower mobilities are stacked at the front of the low mobile matrix zone. This state represents a combina-

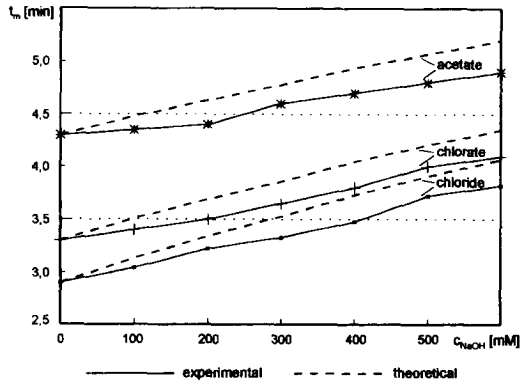

Fig. 6. Comparison of the experimental and the theoretical migration times in the presence of a hydroxide matrix. (The experimental values were taken from Fig. 5a. Parameters for the calculation: $l_0 = 4 \cdot 10^{-3}$ mm; $l_D = 0.7$ m; $\mu_E = 41 \cdot 10^{-9}$ m^2/V·s; $\mu_M = 205 \cdot 10^{-9}$ m^2/V·s; μ_A — see Table 2; $i = 2020$ A/m^2, κ_s was determined by a conductivity measurement and $v_{A,E}$ was calculated from the experimental migration times without a matrix.)

tion of the first two cases of a low and a high mobile matrix. The time of the de-stacking of the analytes can be calculated according to Eqs. 15 and 16.

An example is given in Fig. 7. Fig. 7a shows two electropherograms of inorganic ions with 100 m*M* acetate as the matrix ion and molybdate as the electrolyte. It can be seen that a concentrating effect only occurs for chlorate. By adding 200 m*M* hydroxide to the sample as the second matrix ion, the other analytes also form sharp peaks because a new dominating ITP range is located between the two matrix ions.

Fig. 7b shows the influence of the concentration of the added matrix ion (hydroxide) on the peak heights of the analytes at a constant concentration of the first matrix ion (acetate). As can be seen, the peak heights, and consequently the plate numbers, increase steadily with increasing hydroxide concentration, whereas the peak height of chlorate is nearly constant.

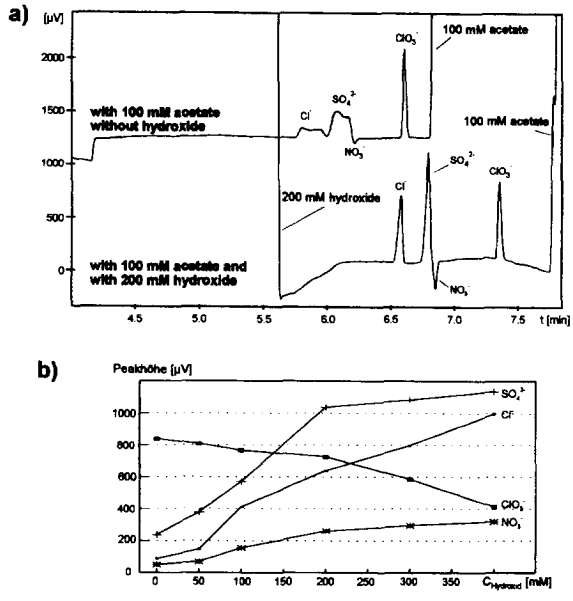

Fig. 7. Influence of two matrices (acetate and hydroxide) on the electropherograms using molybdate as the electrolyte. (a) Electropherograms. (b) Peak heights vs. concentration of hydroxide. Electrolyte, 5 m*M* sodium molybdate, 0.2 m*M* TTAOH (pH 8.8); analytes, 100 μM each, except for acetate (100 m*M*), for hydroxide: 0–400 m*M*; capillary, 69.5 cm to the detector, 76.5 cm total length, 75 μm I.D.; detection, indirect UV (direct UV detection for nitrate), 214 nm; injection, hydrodynamic (0.5 psi, 15 s); device, Beckman P/ACE system 2050.

The reason for this effect is that chlorate lies in the ITP range between the electrolyte molybdate and the matrix ion acetate. Therefore, the de-stacking time of chlorate is independent of the hydroxide matrix and no further stacking effect for chlorate is available by increasing the concentration of the hydroxide matrix. Only by raising the acetate concentration would the ITP time be increased and an improvement in the focussing effect of chlorate be observed.

In contrast to chlorate, the other analytes are in the ITP range built by the hydroxide matrix and the co-ion molybdate. Hence, for these analytes, the influence of the ITP state can be developed continuously by increasing the concentration of the hydroxide matrix.

The advantage of this selected combination of two matrix ions is that the electrolyte can be chosen in a way that its mobility is closely matched to that of the analytes, to improve the electrophoretic separation and to prevent electrodispersive effects.

Another example of the applicability of a second matrix ion using a high mobile chromate electrolyte is shown in Fig. 8. Electropherogram (a) shows a standard without matrix. Here all the ions can be determined. In electropherogram (b) the same standard in the presence of a fluoride matrix can be seen. It is obvious that for phosphate peak-broadening

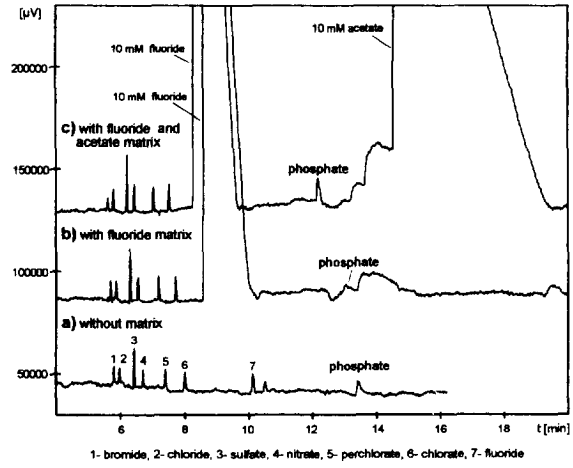

Fig. 8. Influence of a second matrix ion (acetate) on the determination of inorganic ions in the presence of a fluoride matrix. Electrolyte, 7 m*M* chromic acid, 17 m*M* TRIS, 1 m*M* DoTAOH, pH 7.9; analytes, 25 μM each; capillary, 70 cm to the detector, 86 cm total length, 75 μm I.D.; detection, indirect UV, 274 nm; injection, hydrostatic (10 cm, 30 s); device, laboratory-built.

results, because its mobility is out of the mobility range of chromate and fluoride. By adding the matrix ion acetate to the sample, a second ITP state occurs (see Fig. 8c). The first ITP range is formed by the co-ion chromate and the matrix fluoride and leads to the focussing of the analytes, with the exception of phosphate (see also Fig. 4 and Fig. 8b). The second ITP state takes place between the fluoride matrix and the acetate matrix. Due to this ITP state, a stacking process for phosphate results and, therefore, it can be analyzed in the presence of a fluoride matrix.

Therefore, by using the second matrix ion more analytes can be determined simultaneously.

5. Summary

The combination of CZE with an ITP initial state is an excellent way to determine the analyte ions in the presence of a matrix ion without any modification of the CZE apparatus. Therefore, this method is transferable to commercial automatic CZE devices.

Matrix effects in CZE were investigated with several electrolytes and matrix ions. As assumed, an ITP state takes place between the matrix ion and the electrolyte ion before the beginning of the CZE separation. It was shown that the size of the matrix effects is dependent on the mobility and concentration of both the electrolyte and the matrix ion as well as on the length of the sample zone. They act as the leading or terminating ion depending on the mobilities of the matrix ion and the electrolyte co-ion. This ITP mode leads to higher peaks for analytes with mobilities between those of the matrix and the electrolyte ion. In this way, a matrix effect can be an advantage when compared to a common CZE separation, because of increased plate numbers and improved limits of detection of the analytes.

In contrast, analytes with mobilities outside the ITP range are subjected to peak-broadening.

The most unfavourable matrix case exists if the electrolyte and the matrix ion have similar mobilities. In this instance, no ITP state is available. For all analytes peak-broadening results even for matrix concentrations lower than the electrolyte concentration.

Our investigations have also shown that the migration times of the analytes are shifted in the presence of different matrices. If the ITP state takes place between a low mobile matrix and a high mobile co-ion, shorter migration times result for the analytes compared to those found in a pure CZE run. For a high mobile matrix and a low mobile co-ion, however, the analytes are slowed down during the ITP state resulting in higher migration times. It was found that the experimental and the calculated migration times show good agreement.

The ITP range can be shifted by adding a second matrix ion, with an adequate mobility, to the sample solution. In this case, the co-ion does not have a strong influence on the ITP state and can therefore be chosen in a way that it is adjusted for optimum CZE separation conditions.

Furthermore, it was shown that a second matrix ion with appropiate mobility can be used to determine more analytes simultaneously.

6. Symbols

i	current density [A/m^2]
F	Faraday-constant [C/mol]
$\mu_{E,C,M,A}$	mobilities of the co-ion of the electrolyte E, of the counter-ion of the electrolyte C, of the matrix ion M and of the analyte ion A
E	electric field strength [V/m]
$v_{i,j}$	velocity of the ion i in the zone j [m/s]
$c_{M,S}$	concentration of the matrix ion in the sample zone [mol/m^3]
$c_{M,r}$	regulated matrix concentration [mol/m^3]
c_E	concentration of the co-ion of the electrolyte E [mol/m^3]
$\kappa_{S,E,M}$	electric conductivity in the sample zone S, electrolyte zone E and in the regulated matrix zone M [C/m·V·s]
$\kappa_{z(x,t)}$	electric conductivity of boundary z [C/m·V·s]
l_0	injection length of the sample zone [m]
l_r	length of the matrix zone after the regulation process [m]
l_D	length of the capillary up to the detector [m]
l_t	total length of the capillary [m]

M-E	sharp zone boundary of the regulated matrix zone and the electrolyte
M_d	diffuse matrix zone
z	sharp boundary of the matrix zone containing electrolyte

Acknowledgments

The authors thank Beckman Instruments (Munich, Germany) for supporting this work by placing an automatic CZE device P/ACE system 2050 at our disposal.

References

[1] P. Gebauer, W. Thormann and P. Boček, J. Chromatogr., 608 (1992) 47.
[2] P. Jandik and W.R. Jones, J. Chromatogr., 608 (1992) 385.
[3] J. Boden, K. Bächmann, L. Kotz, F. Fabry and S. Pahlke, J. Chromatogr. A, 696 (1995) 321.
[4] J. Romano, P. Jandik, W.R. Jones and P.E. Jackson, J. Chromatogr., 546 (1991) 411.
[5] P. Jandik and G. Bonn, Capillary Electrophoresis of Small Molecules and Ions, VCH Verlagsges., Weinheim, 1993, pp. 189–194.
[6] J. Boden, M. Darius and K. Bächmann, J. Chromatogr. A, 716 (1995) 311.
[7] F.E.P. Mikkers, F.M. Everaerts and Th.P.E.M. Verheggen, J. Chromatogr., 169 (1979) 1.
[8] F.E.P. Mikkers, F.M. Everaerts and Th.P.E.M. Verheggen, J. Chromatogr., 169 (1979) 11.
[9] R.L. Chien and D.S. Burgi, Anal. Chem., 64 (1992) 489A.
[10] D. Kaniansky and J. Marak, J. Chromatogr., 498 (1990) 191.
[11] D.S. Stegehuis, H. Irth, U.R. Tjaden and J. van der Greef, J. Chromatogr., 538 (1991) 393.
[12] D.S. Stegehuis, U.R. Tjaden and J. van der Greef, J. Chromatogr., 591 (1992) 341.
[13] F. Foret, V. Sustacek and P. Boček, J. Microcol. Sep., 2 (1990) 229.
[14] F. Foret, E. Szoko and B.L. Karger, J. Chromatogr., 608 (1992) 3.
[15] L. Krivankova, P. Gebauer, W. Thormann, R.A. Mosher and P. Boček, J. Chromatogr., 638 (1993) 119.
[16] J.L. Beckers and F.M. Everaerts, J. Chromatogr., 508 (1990) 19.
[17] F. Kohlrausch, Ann. Phys. Chem. N.F., 62 (1897) 209.
[18] P. Boček, M. Deml, P. Gebauer and V. Dolnik, in B.J. Radola (Editor) Analytical Isotachophoresis, VCH Verlagsges., Weinheim, 1988.
[19] V. Sustacek, F. Foret and P. Boček, J. Chromatogr., 545 (1991) 239.
[20] L. Gross and E.S. Yeung, Anal. Chem., 62 (1990) 427.
[21] M.W.F. Nielen, J. Chromatogr., 588 (1991) 321–326.
[22] T. Wang and R.A. Hartwick, J. Chromatogr., 607 (1992) 119–125.
[23] F. Foret, S. Fanali, L. Ossicini and P. Boček, J. Chromatogr., 470 (1989) 299.
[24] F. Foret, S. Fanali, A.L. Nardi and P. Boček, Electrophoresis, 11 (1990) 780.
[25] A. Röder and K. Bächmann, J. Chromatogr. A, 689 (1994) 305.
[26] W.R. Jones and P. Jandik, Amer. Lab., 22 (1990) 51.
[27] W.R. Jones and P. Jandik, J. Chromatogr., 546 (1991) 445.
[28] CRC Handbook of Chem. and Phys., 71th ed., CRC Press, Boca Raton, FL, 1991.